11th International Conference on Fast Sea Transportation
FAST 2011, Honolulu, Hawaii, USA, September 2011

Measurements and Computational Predictions of A Deep-V Monohull Planing Hull

T. C. Fu[1], R. Akers[2], T. O'Shea[3], K. Brucker[3], D.G. Dommermuth[3], and E. Lee[1]

[1]Naval Surface Warfare Center, Carderock Division, W. Bethesda, MD, USA
[2]Maine Marine Composites, Portland, ME, USA
[3]SAIC, La Jolla, CA, USA

ABSTRACT

The hydrodynamics of a deep-V planing boat at high Froude numbers is a challenge to measure experimentally and simulate numerically. The U.S. Office of Naval Research has sponsored efforts to develop numerical predictive tools that can be used in the design of high speed craft. Two of these codes are Numerical Flow Analysis (NFA) and POWERSEA. NFA is a high fidelity CFD code requiring supercomputer type resources. It provides turnkey capabilities to model breaking waves around a ship, including both plunging and spilling waves, the formation of spray, and air entrainment. While POWERSEA is an added mass, strip-theory simulation code used to predict performance of planing craft in calm water and in waves. POWERSEA was developed to run on a personal computer and provide a first order assessment of accelerations and loads. To support these efforts, model tests were performed at the Naval Surface Warfare Center Carderock Division. Resistance, sinkage and trim, longitudinal wave cuts, and free-surface topologies were obtained. The model tested was as large as practical (minimizing scaling effects), while still being able to obtain the necessary speed range (6-50 knots full scale). Simulations of the hydrodynamics of the deep-V planing craft were performed utilizing NFA and POWERSEA and compared with the results from the model test.

KEY WORDS

Deep-V, planing craft, CFD

1.0 INTRODUCTION

The qualitative and quantitative characterization of the complex multiphase free-surface flow field generated by a Deep-V monohull planing boat at high Froude numbers is a challenge to both measure experimentally and simulate numerically. Free-Surface Computational Fluid Dynamics (CFD) codes have been developed, primarily to predict the flow around displacement hull ships. Recently the U.S. Office of Naval Research has sponsored efforts to develop numerical predictive tools that can be used in the design of high speed craft. Two of these numerical codes are Numerical Flow Analysis (NFA) and POWERSEA. NFA is a high fidelity computational fluid dynamics code requiring supercomputer type resources while the other tool POWERSEA was developed to run quickly on a personal computer and only provide a first order assessment of accelerations and loads. NFA provides turnkey capabilities to model breaking waves around a ship, including both plunging and spilling breaking waves, the formation of spray, and the entrainment of air. NFA uses a Cartesian-grid formulation with immersed body and volume-of-fluid (VOF) methods. POWERSEA is an added mass, strip-theory planing hull simulation computer code used to predict performance of planing craft in calm water and in waves.

In order to support the development of these codes for predicting the flow around planing craft, a test program was developed to obtain resistance, sinkage and trim, hull pressures, and free-surface topologies on a representative Deep-V planing craft. Due to the complexity of planing craft hydrodynamics, it was desirable to maximize the model size (thus minimizing scaling errors) while still being able to obtain a wide Froude number range (0.31 to 2.5) in a tow tank. The model was tested on Carriage 5 at the David Taylor Model Basin, Naval Surface Warfare Center Carderock Division (NSWCCD), which has a top speed of 50 knots. The basin dimensions are: length of 904 m (2966 ft) and width of 6.4 m (21 ft). The basin has a shallow section with a depth of 3 m (10 ft) and a deep section with a depth of 4.9 m (16 ft). The majority of the experimental measurements were performed in the deep section of the tow tank. The model was tested in both calm water and regular waves over a speed range of 1.78 to 14.2 m/s (5.8 to 46.6 ft/s) corresponding to a Froude number range of 0.31 to 2.5. At planing speeds (+8 m/s), the model was run with the addition of trim tabs at tab angles, of 7 and 13 degrees.

2.0 EXPERIMENT

While the planing craft model test program focused on collecting a wide range of types of measurements for comparison with CFD predictions, the comparison below will focus on (1) resistance, sinkage and trim, (2) wave topology, and (3) flow visualization.

2.1 Model

The Deep-V planing hull chosen for this test program was representative of a monohull planing hull craft. The model size was chosen to be as large as practical for testing on Carriage 5 at NSWCCD to minimize scale effects, while covering as wide a speed range as possible, up to 14 m/s (46.6 ft/s). A Deep-V monohull planing craft model was built of pine lifts in the model shop at NSWCCD. The model was painted yellow and station lines were added to the hull bottom and sides. A checkerboard grid comprised of

one inch squares was applied to the hull bottom, and waterline marks were added to the station lines on the hull sides as visual aids for calculation of wetted surface area.

In order to collect measurements in both calm water and in waves, static and dynamic ballasting of the model was performed. Additionally, in contrast to displacement vessels with fixed propulsors and rudders, planing craft are typically propelled by steerable propulsors – outboard motors, stern drives/outdrives, waterjets, etc. The thrust provided by these propulsors has horizontal and vertical components, and the vertical component becomes significant as the craft trims. Additionally, the thrust line can be at or even below the keel line. Both the horizontal and vertical thrust forces anticipated on a full-scale craft must be accurately represented at model scale. However, only horizontal force is applied to the model. To simulate the vertical component of the thrust, an upward force, an amount of weight equivalent in magnitude to the anticipated vertical force component is removed from the model without shifting the longitudinal center of gravity (LCG). To accurately represent application of propulsor thrust to a full-scale craft, the model should be towed at the point at which thrust is applied - the intersection of the LCG and the thrust (shaft) line. In most cases, a planing model cannot be towed at this location, since the thrust line is too low. The model is still towed at the LCG, but at a higher location, creating a moment which does not exist at full scale. This artificial moment was compensated while ballasting the model.

Table 1. Test Matrix - First Testing Period

Test number	Sea State	Description	Data Collected
1	Calm	Check out test	
2	Calm	8.9, 11.8 m/s, 7° tabs	RST
3	Calm	8.9 m/s, 13° tabs	RST
4	Calm	3, 8.9, 11.8 m/s , 13° tabs	RST
5	Calm	1.8, 2.4, 3 m/s, No tabs	RST
6	Calm	Trim checks	
7	Calm	8.9, 11.8 m/s, 13° tabs	RST
8	Calm	8.9, 11.8 m/s, 13° tabs	RST
9	Calm	8.9, 11.8 m/s, 7° tabs	RST
10	Calm	3, 14.2 m/s 13° tabs	RST

Notes: RST: resistance, sinkage and trim, Tests #11-14 were in waves tests.

Model testing was divided into two test periods. The first period focused on the resistance and sinkage and trim measurements; the second test period was the free-surface wave field measurement. Resistance and sinkage and trim were also measured during the second test period to insure reproducible results. Tables 1 and 2 show the test conditions performed in each test period.

Table 2. Test Matrix - Second Test Period

Test number	Sea State	Description	Data Collected
15	Calm	1.8 m/s, No tabs	RST, ST, QVIZ
16	Calm	1.8, 3 m/s, No tabs	RST, ST, QVIZ
17	Calm	1.8, 3 m/s, No tabs	RST, ST, QVIZ
18	Calm	8.9 m/s, 13° tabs	RST, ST, QVIZ
19	Calm	8.9 m/s, 7° tabs	RST, ST, QVIZ
20	Calm	8.9 m/s, 7° tabs	RST, ST, QVIZ
21	Calm	8.9 m/s, 13° tabs	RST, ST, QVIZ
22	Calm	11.8 m/s, 13° tabs	RST, ST, QVIZ
23	Calm	8.9 m/s, No tabs	RST, ST, QVIZ
24	Calm	8.9 m/s, No tabs	RST, ST, QVIZ
25	Calm	11.8 m/s, 13° tabs	RST, ST, QVIZ
26	Calm	2.4 m/s, No tabs	RST, ST, QVIZ
27	Calm	1.8, 2.4, 3 m/s, No tabs	RST, ST, QVIZ

Notes: RST: resistance, sinkage and trim; ST: stern topography; QVIZ: quantitative visualization

Additionally at each speed, wetted-bottom area was determined using underwater photos and the checkerboard grid (see Figure 1a), and the wetted side area was determined using side photos (Figure 1b).

a)

b)

Fig. 1. Sample images used to compute wetted surface area: a) the bottom view and b) the side view at a speed of 8.9 m/s (29.2 ft/s) and 7 degree trim tab angle.

3.0 EXPERIMENTAL RESULTS

3.1 Resistance, Trim, and Heave

The averaged resistance (drag), trim angle, and heave at the tow post are shown in Figures 2-4. As can be seen there is enormous variation in values at the model speed of 2.96 m/s (9.7 ft/s). At this speed, the model is starting the transition from displacement to planing speed. The addition of trim tabs increases drag at higher speeds (drag is higher for 13 degree tabs than 7 degree tabs), and lowers trim, as expected.

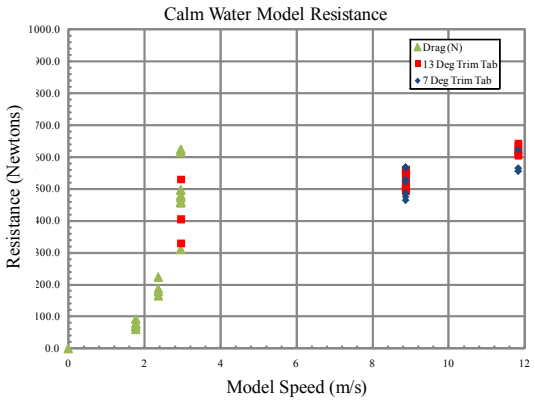

Fig. 2. Model resistance versus speed, with and without trim tabs (7 and 13 degree tab angle), in calm water.

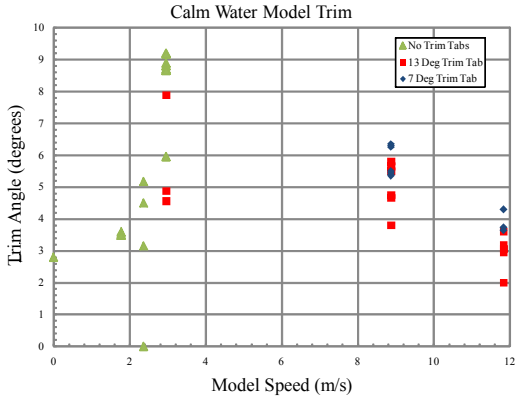

Fig. 3. Model trim versus speed, with and without trim tabs (7 and 13 degree tab angle), in calm water.

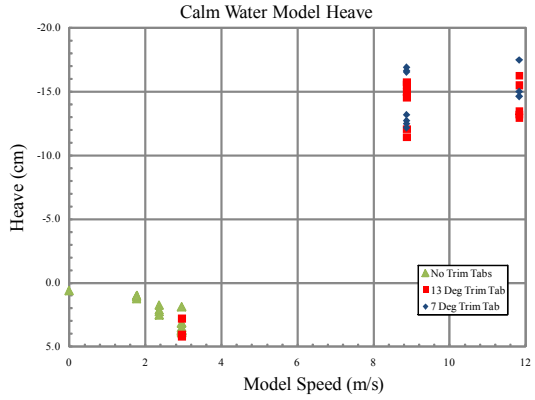

Fig. 4. Model heave versus speed, with and without trim tabs (7 and 13 degree tab angle), in calm water. Heave is negative upward, positive downward.

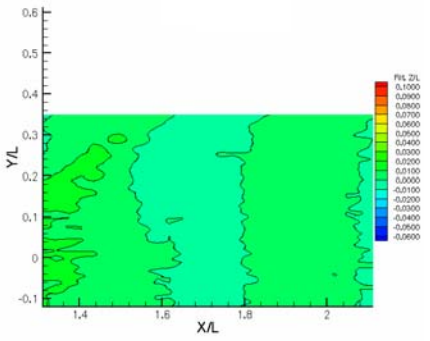

a) 1.8 m/s (5.8ft/s)

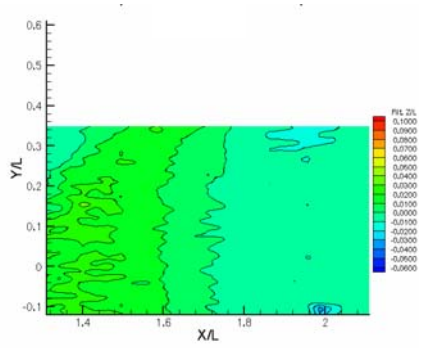

b) 2.4 m/s (7.8 ft/s)

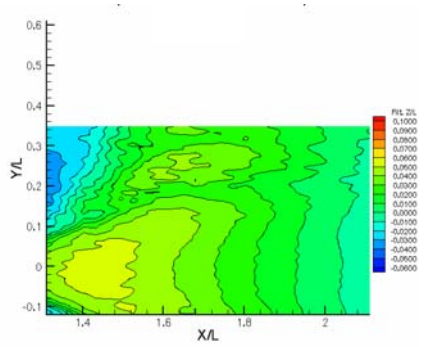

c) 3 m/s (9.7 ft/s)

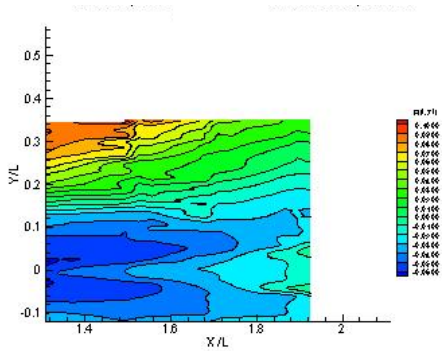

d) 9 m/s (29.2 ft/s)

Fig. 5. Stern topologies for model speeds of 1.8, 2.4, 3, and 9 m/s (5.8, 7.8, 9.7 and 29.2 ft/s), no trim tabs.

3.1 Surface Topology

Figure 5 shows the stern topologies for four speeds of 1.8, 2.4, 3, and 9 m/s (5.8, 7.8, 9.7 and 29.2 ft/s) with no trim tabs. There is little variation transversely for the 1.8 and 2.4

m/s (5.8 & 7.8 ft/s) speeds. At 3 m/s (9.7 ft/s), the flow field varies some in Y/L at small X/L, but as X/L increases the topology becomes fairly homogeneous with respect to Y/L.

The bow wave of Deep-V monohull planing boats is typically characterized by the large spray sheets. Details of this feature are shown in Figures 6 and 7. Figure 6 shows the bow wave generated by the model at a speed of 3 m/s (9.7 ft/s). Figure 7 is an image of the bow wave spray region illuminated by laser sheet, note the turbulent thin fluid sheet generated by the bow wave.

Fig. 6. Bow wave generated by a Deep-V planing hull model at a speed of 3 m/s (9.7 ft/s).

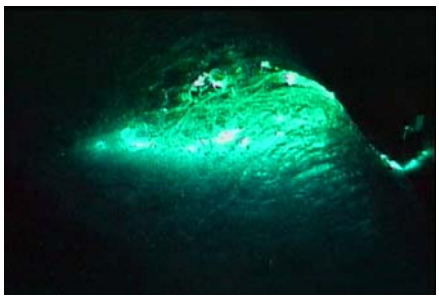

Fig. 7. The spray region generated by the bow wave of Deep-V planing boat model illuminated by a laser sheet.

Quantitative Visualization (QVIZ), a laser sheet optical measurement technique, was utilized to measure the time-averaged transverse profiles of free surface elevation. Figures 8-11 show the time average profiles at 9 m/s (29.2 ft/s), for a number of axial locations. The RMS for each point measured is also shown for points where sufficient information was available. The regions with large RMS values are regions of large unsteadiness/breaking. Note that due to the large axial separation between profiles, no attempt was made to generate a contour map of the free-surface elevation from this data

4.0 NUMERICAL COMPUTATIONS – POWERSEA

POWERSEA is an added mass strip-theory planing hull simulation computer code used to predict performance of craft in calm and rough water. The program is a 2-1/2 dimension simulator, in that it combines cross-flow lift, in the form of impacting wedges and cross-flow drag, with longitudinal flow lift in the form of panel codes implemented upon buttock lines. It is a continuation of the work pioneered by Zarnick (1978, 1979) at NSWCCD. The developer of POWERSEA has published several papers on its capabilities and limitations. POWERSEA has had several revisions since its initial issue.

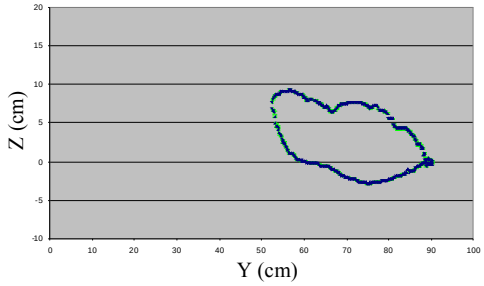

Fig. 8. Time-averaged bow wave profile at Station 7 generated by a Deep-V planing craft model at a speed of 9 m/s (29.2ft/s), no tabs.

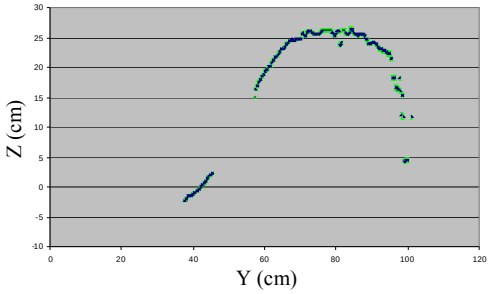

Fig. 9. Time-averaged bow wave profile at Station 10 generated by a Deep-V planing craft model at a speed of 9 m/s (29.2ft/s), no tabs.

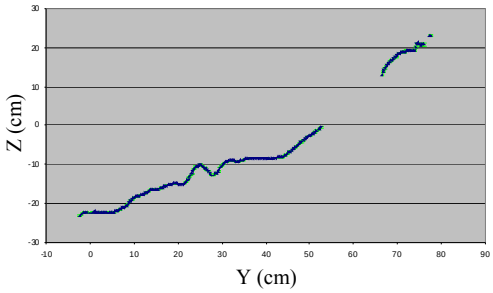

Fig. 10. Time-averaged bow wave profile at Station 12.4 generated by a Deep-V planing craft model at a speed of 9 m/s (29.2ft/s), no tabs.

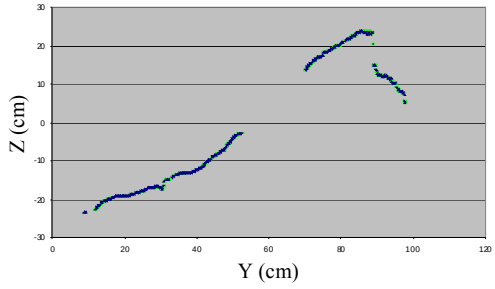

Fig. 11. Time-averaged bow wave profile at Station 13 generated by a Deep-V planing craft model at a speed of 9 m/s (29.2ft/s), no tabs.

4.1 Algorithms

4.1.1 Geometry

Traditionally, an analysis model for low aspect ratio strip theory consists of a keel line and a chine line. Each section consists of a straight line from the keel to the chine, and then an unbounded vertical line from the chine upward. All dynamic forces in a pure low aspect ratio strip theory

algorithm are derived from transverse flow derived from impacting wedge theory or crossflow drag theory.

In order to model more complicated hulls, POWERSEA models both sections and buttock lines. Starting with a set of surfaces, POWERSEA tessellates a set of user-supplied surfaces to create a section/buttock mesh. The offset points that make up each section and buttock line are filtered to eliminate negative deadrise sections and buttock lines with negative camber. During a meshing command, spline curves are created for fast evaluations of draft, girth, wetted beam and sectional centroid, and for panel pressures from ideal flow calculations along buttock lines

4.1.2 Regions of Simulation

POWERSEA has multiple algorithms to simulate sections of a planing hull. The regions of a planing hull are called "Chines-Dry," from the point where the keel is first wet until the longitudinal point where the chine is wet, and "Chines-Wet," covering the entire longitudinal range for which the transverse jet touches the chine. There is a pile-up phenomenon in which the water level on the sides of the boat rises above the calm water line. This extends the length of the chines-wet region (refer to Figures 12 & 13). The chines-dry region is modelled using impacting wedge theory, and the chines-wet region is modelled using crossflow drag theory. Buoyancy and viscous drag are calculated over both regions. A buttock flow algorithm predicts pressures that augment the impacting wedge and crossflow drag forces. This algorithm is applied to the entire wetted surface.

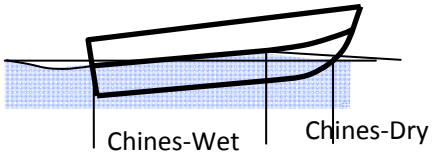

Fig. 12. Regions of pressure on a planing boat.

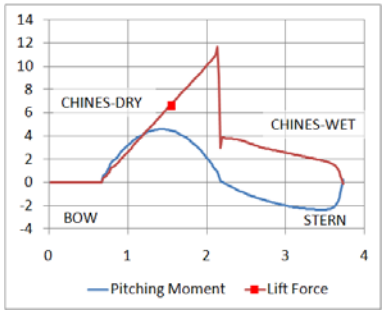

Fig. 13. Sectional dynamic lift and pitching moment from impacting wedge and from crossflow drag.

4.1.3 Wetted Beam

A v-bottomed planing hull forces water to "pile up" transversely along the sections, effectively increasing the submergence of each section. POWERSEA incorporates a quasi-steady-state regression model for the wetted beam as a function of calm water beam and deadrise. Various theories as to steady state pileup have been proposed, including a recent theory published by Vorus (1996). To decrease the computer time required to calculate the wetted beam at each section, a regression model was created based on published curves that document Vorus's results. Figure 14 is a chart displaying three different models for wetting factor. Overlaid on the chart is a plot of results from a simple quadratic regression model using in POWERSEA.

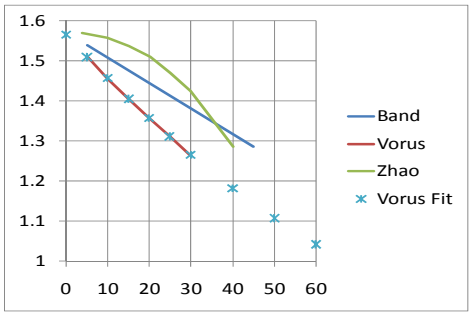

Fig. 14. Wetting Factor to convert calm water draft into draft including pile up. POWERSEA uses a regression model for efficient computation, labelled as "Vorus Fit".

4.1.4 Added Mass

Following the work of Martin (1973), Zarnick (1978, 1979) developed a mathematical formulation for the instantaneous forces on a planing craft. In Zarnick's method a planing craft is modeled as a series of strips or impacting wedges. Zarnick derived the normal hydrodynamic force per unit length as:

$$f = -\left\{\frac{D}{Dt}(m_a V) + C_{D,c}\rho b V^2\right\}$$

$$\text{where } \frac{D}{Dt}(m_a V) = m_a \dot{V} + \dot{m}_a V - \frac{\partial}{\partial \xi}(m_a V)\frac{d\xi}{dt}$$

The first time in brackets is the substantial derivative of the momentum, and the second term is crossflow drag. The added mass and crossflow drag are evaluated at each time-step.

$$\text{Added Mass } (m_a) = Cm' * (\pi/2 * \rho * b_{CALM}{}^2)$$

where b_{CALM} is the effective calm water half beam and Cm' is an added mass coefficient that relates added mass to wetted beam. The added mass coefficient can be computed from a second added mass coeffient, Ka, which relates added mass to the calm water beam.

$$Cm' = Ka * WetFactor^2$$

$$Ka = Ka(\beta_{GLOBAL})$$

Both the wetting factor and the added mass coefficient Ka depend on deadrise. Recent theories from Vorus (1996) and Savander (2002) have been shown to give promising results, and POWERSEA supports both of these theories. Figure 15 is a plot of the added mass coefficient Cm' from both Vorus's and Savander's theories. A set of points calculated using the POWERSEA regression model are plotted on top of the Vorus/Savander data.

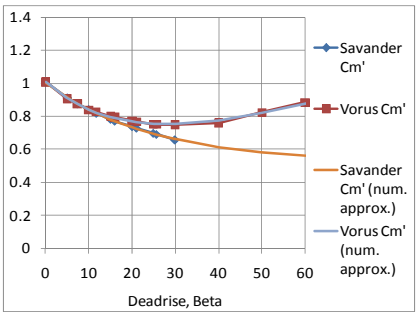

Fig. 15. Added mass coefficient, Cm' versus global deadrise angle β.

Large angle deadrise (β_{GLOBAL}) is used in this formulation. β_{GLOBAL}) is defined as the slope of the line from the keel to the outer point of the instantaneous wetted surface. The time derivative of the added mass can be calculated using the chain rule:

$$\partial m_a / \partial t = \pi /2\ \rho\ \{\ \partial Cm'/\partial\beta_{GLOBAL} * \partial\beta_{GLOBAL}/\partial t * b_{CALM}{}^2 + Cm' * 2 * b_{CALM} * \partial b_{CALM} / \partial t\ \}$$

$$\partial Cm' / \partial\beta_{GLOBAL} = \partial Ka/ \partial\beta_{GLOBAL}\ WF^2 + 2\ Ka\ WF * \partial WF / \partial\beta_{GLOBAL}$$

$$\partial\beta_{GLOBAL} / \partial t = \partial\ \beta_{GLOBAL} / \partial\ d_{WET} * \partial\ d_{WET} / \partial\ t$$

$$\partial\beta_{GLOBAL} /\partial d_{WET} = \partial \arctan(b_{WET} / d_{WET})/ \partial d_{WET} = 1/ (1+(b_{WET}/d_{WET})^2) * \partial(b_{WET}/d_{WET})/\partial d_{WET} = -1/(1+(b_{WET} / d_{WET})^2) * b_{WET} / d_{WET}{}^2$$

$$\partial b_{CALM} / \partial t = \partial b_{CALM} / \partial d_{SECTION} * \partial d_{SECTION} / \partial t$$

Where:

WF = Wetting factor
b_{WET} = (effective) Wetted half-beam
$d_{SECTION}$ = Calm sectional draft
d_{WET} = Wetted sectional draft

The partial derivative of the wetting factor (WF) and the added mass coefficient (Ka) with respect to global deadrise, β_{GLOBAL}, can be calculated directly from the regression models.

The POWERSEA algorithm also requires the partial derivative of added mass with respect to the boat longitudinal axis, ξ. As the boat geometry is specified by the user and is not necessarily smooth, this derivative is calculated numerically.

4.1.5 Crossflow Drag

In the chines-wet region the wetted beam is fixed at the chine, so the added mass becomes constant. Accordingly the added mass model of dynamic force is inadequate in this region. To augment the added mass model, a semi-empirical crossflow drag model is employed in the chines-wet region. This model was created by analyzing quasi-static pressure distributions collected on models (Kapryan, 1955) and a full size boat (Royce, 2001).

4.1.6 Buoyancy and Viscous Drag

Viscous drag is approximated by finding the mean wetted length of the hull, calculating a Reynold's number and then adding the wetted surface contributed by each section. The sectional wetted surface is calculated from the mesh by integrating the girth over the section thickness. The pitching moment created by viscous drag is calculated by assuming that the drag is applied at one-half of the wetted draft of each individual section.

Buoyancy is calculated by integrating the submerged area of each section. For buoyancy purposes the submergence is defined with respect to the calm water surface, not to the pileup surface. The contribution to the pitching moment that results from sectional buoyancy is calculated using the instantaneous centroid of each section.

4.1.7 Buttock Flow

In regions of a hull where there is significant complex compound curvature the impacting wedge algorithm underpredicts the hydrodynamic forces. This is especially important in modelling boats with convex sections near the bow, as much of the dynamic force in this area arises from buttock flow. To address this problem, POWERSEA uses linear panel theory to precalculate a matrix of pressure coefficients along a representative set of buttock lines. For each section a matrix of pressure coefficients can be indexed by instantaneous draft, trim and half-beam. A quadratic interpolation scheme is used to extract instantaneous pressure coefficients for each section at each time step in the simulation. A blending function based on the longitudinal and transverse curvature at the half-beam point of each station is used to combine the dynamic forces from buttock flow and crossflow.

4.2 Model of Generic Planing Hull

A Rhino 3D model of a generic planing hull was provided. This model was converted to IGES format and imported into POWERSEA. The POWERSEA model is shown below in Figure 16.

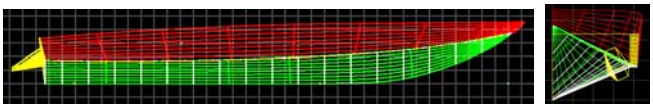

Fig. 16. POWERSEA model of generic planing hull.

The upper (red) surface shown if Figure 16 is the side of the vessel and is not included in the planing calculations. The lower hull surface and the chine flat are designated as the planing surface. Representative stations calculated by POWERSEA are drawn in white. The station geometry extends across the lower hull surface and the chine flat.

4.3 Simulation Results -- POWERSEA

Table 3 shows the results of the POWERSEA calculation and the average of the model test data. One can see that generally the predictions for trim, heave and resistance agree reasonably well.

Table 3. POWERSEA RESULTS

Model Scale Speed (m/s)	Trim Tab Angle (deg)	Weight (N)	LCG forward from the Transom (m)	VCG (cm)	Pitch Gyradius (cm)	Heave (cm)	Pitch (degr)	Resistance (N)
8.90	7	3183.1	1.15	23.5	89.3	-8.04	5.7	540.65
8.90	13	3094.1	1.15	23.3	90.7	-6.33	4.3	569.12
8.90	13	3150.6	1.17	23.5	89.6	-6.06	4.3	590.46
8.90	7	3150.6	1.17	23.5	89.6	-7.86	5.5	542.12
8.90	0	3150.6	1.09	24.5	85.4	-11.11	7.0	552.54
11.80	7	3183.1	1.15	23.5	89.3	-10.34	3.6	677.95
11.80	0	3150.6	1.09	24.5	85.4	-13.58	5.0	615.77

5.0 NUMERICAL COMPUTATIONS - NFA

5.1 Formulation

Numerical simulation of the flow field around a Deep-V planing craft was performed utilizing the Numerical Flow Analysis (NFA) code. NFA provides turnkey capabilities to model breaking waves around a ship, including both plunging and spilling breaking waves, the formation of spray, and the entrainment of air. NFA uses a cartesian grid formulation with a cut-cell representation of the hull and volume-of fluid (VOF) interface capturing of the free surface. A complete discussion of the formulation of NFA can be found in Brucker, O'Shea & Dommermuth (2010).

5.2 Results

Length scales are normalized by L_o, the length between perpendiculars. Velocity scales are normalized by U_o, the ship speed. As a result, time is normalized by $T_o = L_o/ U_o$. Forces are normalized by $\rho_\omega\ U_o{}^2\ L_o{}^2$, and moments are normalized by $\rho_\omega\ U_o{}^2\ L_o{}^3$, where ρ_ω =1000kg/m^3 is the density of water. The Froude number is $Fr = U/\sqrt{gL_o}$ where g =9:80665m/s^2, acceleration of gravity. Table 4 provides the normalization for the three simulations of the Deep-V model with 13-degree trim tabs at 8.91 m/s, 11.88 m/s and 14.38 m/s model scale. These speed and trim tab combinations are represented in test numbers 4 and 10 in Table 1

5.2.1 Gridding

Table 5 provides the dimensions of the computational domain for the simulations and the smallest grid spacing. For example, X_{min} and X_{max} respectively denote the minimum and maximum offsets along the x-axis in normalized units. Similarly, Δx_{min} and Δx_{max} are respectively the minimum and maximum grid spacings along the x-axis in normalized units. Note that the grid is stretched along the Cartesian axes. Grid points are clustered near the ship and the mean waterline. Reflective boundary conditions are used at the tops, bottoms, sides, and fronts of the computational domains. To help waves smoothly transition out of the back of the domain, Orlanski exit boundary conditions are used downstream of the ship along the x-axis. Free-stream velocity is in the negative x direction.

Table 4. Normalizations.

Experimental Test #	L_o (m)	U_o (m/s)	T_o (s)	Fr
4	3.301	8.91	0.370	1.566
4	3.301	11.88	0.278	2.088
10	3.301	14.38	0.229	2.528

Table 5. Deep-V Gridding Details

	X	Y	Z	Δx	Δy	Δz
Min	0.5	0.0	0.5	1.2E-3	9.1E-4	1.0E-3
Max	-2.5	-1.0	-1.0	1.2E-2	2.0E-2	4.0E-2

5.2.2 Panelization

Figure 17 shows the panelizations that were used for Deep-V simulations. This geometry was carefully redone to model the fine detail of the Deep-V planing hull, including all the steps, spray rails and trim tabs. The panel densities are higher in regions of high curvature. The panelization is coarse in regions where the hull geometries are flat. The panel density does not affect the accuracy of the calculation of signed-distance function that NFA uses internally to represent a ship.

Fig. 17. Deep-V panelization

Signed-distance functions are used to represent ship hulls internally within NFA. First, the shortest distance between a point in the cartesian grid to the ship hull is calculated. Then this distance is assigned a negative distance if the point is within the hull and a positive distance if the point is outside the hull to create a signed-distance function. A zero distance corresponds to a point that is on the ship hull.

The sinkage and trim of the model were deduced from the model test experiments. Only relative sinkage was recorded for each run, so the absolute sinkage was calculated from the static trim and displacement. Using 3D modeling software, the boat was oriented at the static trim and then moved vertically until the weight of the displaced volume equaled the weight of the boat. From this baseline position the relative sinkage at the bow and stern was applied. This method introduces additional errors into the sinkage and trim. Planing boats are especially sensitive to slight changes in sinkage and trim, which can greatly affect force calculation as discussed is the subsequent forces section.

5.2.3 Simulations

The numerical simulations were run on the SGI ICE on 576 CPUs for over 20,000 time steps with a non-dimensional time step Δt=0.0025. The results of the 14 m/s (46.8 ft/s), 11.8 m/s (39 ft/s) and 9 m/s (29.2 ft/s) simulations can be seen in Figures 18, 19, and 20. These figures show two isosurfaces of the time-averaged volume fraction taken over 4000 time steps or 1 boat length. The opaque blue isosurface represents a volume fraction of 0.8 while the transparent white isosurface represents a value of 0.05. Spray is highlighted in these plots since the averaged volume fraction is diffuse in the presence of highly time-varying free surface. For comparison, Figure 21 shows a photograph from the 9 m/s (29.2 ft/s) experimental test taken from approximately the same angle. Qualitative structure of the wake and spray generation agree remarkably well. We note that NFA's spray does not carry as far downstream due to grid stretching in the x and y directions. The spray can only exist as long as there are cells small enough to resolve it.

Whisker-probe data provides an excellent way to validate NFA's free-surface topology in the region behind the stern. Figure 22 shows the experimental data plotted on top of the NFA simulation for the 9 m/s (29.2 ft/s), 13 degree trim-tab case. The whisker-probe stern topology is outlined with a black box. The simulation compares extremely well to the

experiments for such a complex flow and difficult to measure flow field.

Fig. 18. NFA simulation of Deep-V at 14 m/s (46.8 ft/s).

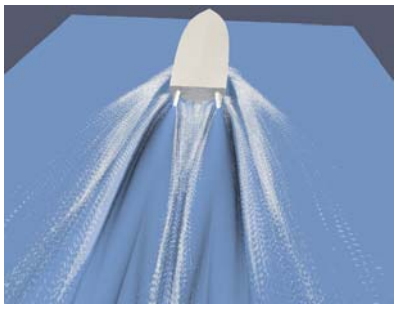

Fig. 19. NFA simulation of Deep-V at 11.8 m/s (39 ft/s).

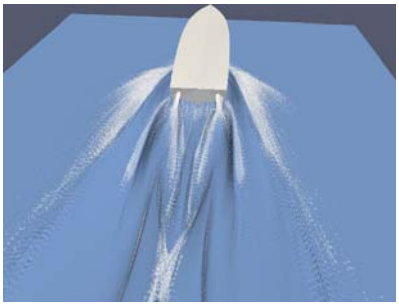

Fig. 20. NFA simulation of Deep-V at 9 m/s (29.2 ft/s).

Fig. 21. Deep-V experimental photograph.

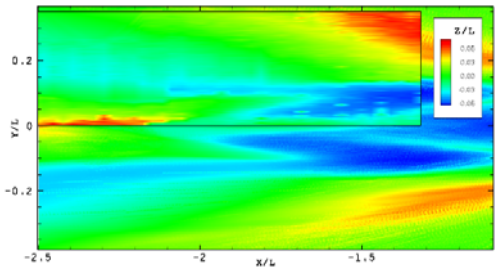

Fig. 22. Comparison of whisker-probe data & NFA results for 9 m/s (29.2 ft/s).

5.2.4 Pressure

Figure 23 shows the pressure from NFA interpolated onto the panelized representation of the hull. The bulk of the pressure acting on the hull is concentrated at the contact line as is typical in planing craft. The trim tabs also carry a large amount of pressure. The shallow angle between the tabs and water's surface means the majority of the force is orthogonal to the drag, which makes them effective at changing the trim without adding a disproportional amount of resistance. The distribution of pressure changes with speed. As speed increases the trim of the boat decreases and the dynamic lift pushes the hull out of the water.

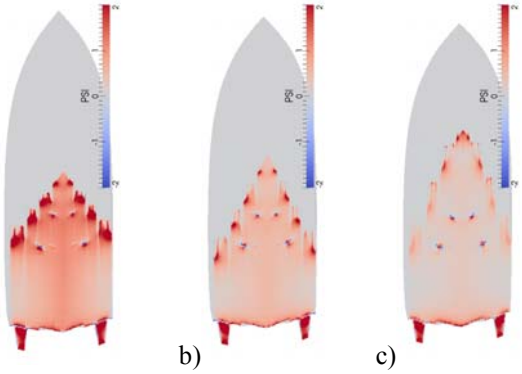

Fig. 23. NFA prediction of pressure on the Deep-V (a) 9 m/s (29.2 ft/s), (b) 11.8 m/s (38 ft/s), (c) 14 m/s (46.8 ft/s).

5.2.5 Forces

Forces on a model are typically broken into two parts, wave-making and viscous drag. Integrating the pressure on the hull gives us the wavemaking portion of the force. The viscous portion is calculated from the wetted surface area, Reynolds number and the ITTC flat plate friction equation (see Dommermuth, et al. 2006 and O'Shea, et al., 2008). Plots of the X and Z components of these forces are given in Figure 27. The drag measurements, represented by the red line, compare quite well with NFA's X force measurements, represented by the black line. The model experiment did not measure Z force, so the reported static displacement of the model is shown as the pink line in the figure. It should be noted that there is some uncertainty with this number. The typical behavior of a planing craft is to reduce trim and reduce sinkage as speed increases. The 14 m/s (46.8 ft/s) case actually had more sinkage than the 11.8 m/s (38 ft/s) case, which could be due to additional weight being added to help with thrust unloading as described earlier in the experimental section. The variability of the Z forces could also be attributed to the errors introduced by estimating the sinkage and trim as discussed in the previous section.

6.0 CONCLUSIONS

The model test of a Deep-V, monohull model provided a comprehensive set of planing craft data for the validation of CFD codes. The test generated several unique types of data, including traditional resistance and trim measurements, hull pressures, and multiple quantifications of the flow field itself. Each of these data types represented a specific interpretation of planing craft hydrodynamics, and

collectively, this information should prove valuable as CFD codes are developed and evaluated for planing craft applications.

Two simulation codes were demonstrated. POWERSEA, a fast added mass strip-theory planing hull simulation computer code and Numerical Flow Analysis (NFA) a higher-order code utilizing a Cartesian grid formulation with a cut-cell representation of the hull and volume-of fluid (VOF) interface capturing code.

REFERENCES

Brucker, K. A., O'Shea, T. T., & Dommermuth, D., (2010), "Numerical Simulations of Breaking Waves -Weak Spilling to Strong Plunging," 28th Symp. on Naval Hydrodynamics, Pasadena, CA.

Dommermuth, D. G., O'Shea, T. T., Wyatt, D. C., Sussman, M., Weymouth, G. D., Yue, D. K., Adams, P., & Hand, R., (2006), "The Numerical Simulation of Ship Waves Using Cartesian-Grid and Volume-of-Fluid Methods," 26th Symp. on Naval Hydro., Rome, Italy.

Kapryan, W. J. and Boyd, G. M., Jr., (1955), "Hydrodynamic Pressure Distributions Obtained During a Planing Investigation of Five Related Prismatic Surfaces," National Advisory Committee for Aeronautics (NACA).

Martin, M., (1973), "Theoretical Determination of Porpoising Stability of High Speed Planing Boats," Journal of Ship Research, pp 32-53.

O'Shea, T. T., Brucker, K. A., Dommermuth, D. G., & Wyatt, D. C., (2008), "A Numerical Formulation for Simulating Free-surface Hydrodynamics," Proc. of the 27th Symp. on Naval Hydrodynamics, Seoul, Korea.

Royce, Richard A., (2001), "2-D Impact Theory Extended to Planing Craft with Experimental Comparisons," Ph.D. thesis, NAME, University of Michigan.

Savander, Brant R., Scorpio, Stephen M., and Taylor, Robert K., (2002), "Steady Hydrodynamic Analysis of,Planing Surfaces," Jour. of Ship Res., Vol. 46, No. 4, pp. 248-279.

Vorus, W.S., (1996), A Flat Cylinder Impact Theory for Analysis of Vessel Impact Loading & Steady Planing Resistance." Jour. of Ship Res., Vol. 40, No. 2, pp. 89-106.

Zarnick, Ernest E., (1978), "A Nonlinear Mathematical Model of Motions of a Planing Boat in Regular Waves," David W. Taylor Naval Ship Research and Development Center, DTNSRDC 78/032.

Zarnick, Ernest E., (1979), "A Nonlinear Mathematical Model of Motions of a Planing Boat in Irregular Waves," David W. Taylor Naval Ship Research and Development Center, DTNSRDC/SPD 0867 01.

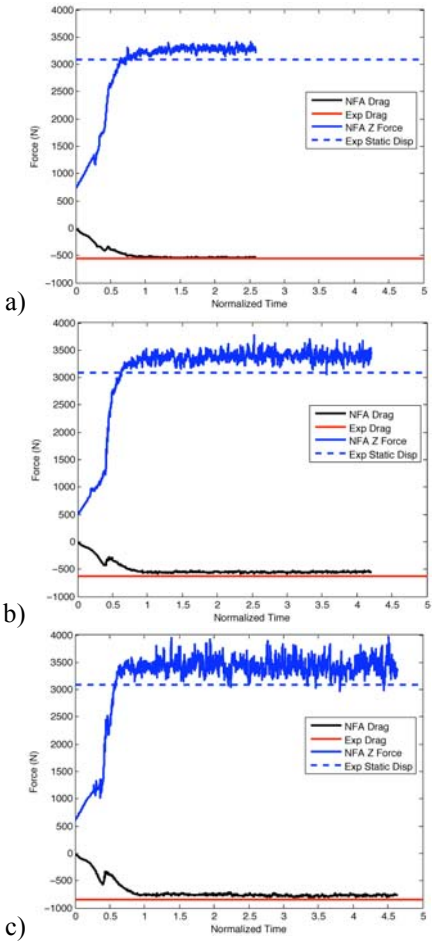

Fig. 24. Deep-V Force Comparison (a) 9 m/s (29.2 ft/s), (b) 11.8 m/s (38 ft/s), (c) 14 m/s (46.8 ft/s).

ACKNOWLEDGEMENTS

The Office of Naval Research supports this research. Dr. Steve Russell supported the NFA research and Dr. L. Patrick Purtell the analysis and reporting of the testing effort. SAIC IR&D also supported the development of NFA. This work is also supported in part by a grant of computer time from the Dept. of Defense High Performance Computing Modernization Program. The numerical simulations were performed on the SGI ICE at the U.S. Army Engineering Research and Development Center. The authors would also like to acknowledge the contributions of those associated with the model test program: James R. Rice, Donnie Walker, Deborah Furey, Bill Boston, and Peter Congedo.